LUNAR REGOLITH EVOLUTION RATES DERIVED FROM THERMOPHYSICAL PROPERTIES

Carlton Allen[1], Rebecca Ghent[2], Cailin Gallinger[3], and David Paige[4]
[1]NASA (retired) callen5126@comcast.net, [2]Planetary Science Institute, Tucson, AZ rghent@psi.edu, [3]University of Toronto, Toronto, Canada cailingallinger@gmail.com, and [4]UCLA, Los Angeles, CA dap@moon.ucla.edu.

Introduction: The lunar regolith evolved over hundreds of millions of years from impacts on a wide range of scales that comminuted and buried surface material. Evolution rates, derived from Apollo cores, are restricted to small areas and local events. This study uses the thermophysics of crater ejecta to constrain evolution rates on a scale of kilometers.

Apollo Cores: The regolith was cored to depths as great as 2 m by the Apollo astronauts. Cores were meticulously dissected, and subsamples dated, to understand regolith evolution. The cores display multiple cm-scale layers, distinguished by composition and *in situ* exposure age. Ages increase with depth, supporting a model of repeated burial by localized impact events. A correlation, derived from Apollo 15, 16, and 17 cores, shows a log relationship, with an age of ~ 100 my corresponding to a depth of 10 cm [1,2].

Remote Sensing: Remote sensing data, from Earth and lunar orbit, provide an estimate of regolith evolution rates at a much larger scale. This study encompasses the Aristarchus plateau. Observations include radar and visible images combined with regolith temperatures.

Aristarchus: The Aristarchus plateau is a 170 by 200 km block of highland crust that rises 2 km above Oceanus Procellarum. The 40 km diameter Aristarchus crater dominates the SE corner of the block. Estimates of the crater age range from 130 – 189 my [3]. A pyroclastic deposit with a depth of ~ 10 m covered much of the plateau approximately 3.5 Ga ago [4]. By analogy to the Taurus-Littrow pyroclastic deposit samples, the Aristarchus pyroclastics are likely dominated by 10 - 100 μm diameter glass beads. The study area is located in the western section of the deposit near Schroter's Valley, a large sinuous rille.

Radar: Campbell *et al.* [5] studied the Aristarchus plateau with Earth-based radar at wavelengths of 12.6 and 70 cm. The radar penetration depth in lunar soil is ~ 10 - 20 wavelengths.

Visible Light: The LRO camera (LROC) system includes a panchromatic narrow-angle camera (NAC) and a wide-angle camera (WAC) that images the Moon using seven filters spanning the visible and near-IR [6]. These images sample only the very surface of the Moon. Normalized reflectance WAC images (643 nm) are taken when the sun is directly overhead, emphasizing albedo differences on the lunar surface.

Thermophysical: Diviner is a near/thermal IR mapping radiometer on LRO, designed to measure temperatures on the lunar surface with a precision of better than 1 K [7]. Over the lunar diurnal cycle, the thermal wave penetrates to a depth of ~ 10 - 20 cm. Only material within this "skin depth" undergoes temperature variations on a diurnal timescale. Hayne *et al.* [8] used Diviner data to map thermophysical properties, expressed by the "H-parameter" (units of m), which is inversely proportional to thermal inertia.

Observations: Radar, visible light, and temperature data present complementary insights into features within the Aristarchus pyroclastic deposit.

Radar: Campbell *et al.* [5] noted numerous km-scale streaks across the study area that display enhanced radar reflectivity (Fig. 1). The streaks are generally radial to the Aristarchus crater, ~ 150 km to the SE. These authors concluded that the radar was sensing rocks larger than ~ 2 cm, formed by impacts of blocks ejected during the cratering event. The streaks are apparent in 12.6 cm radar images, which are sensitive to depths as great as 1.3 - 2.6 m.

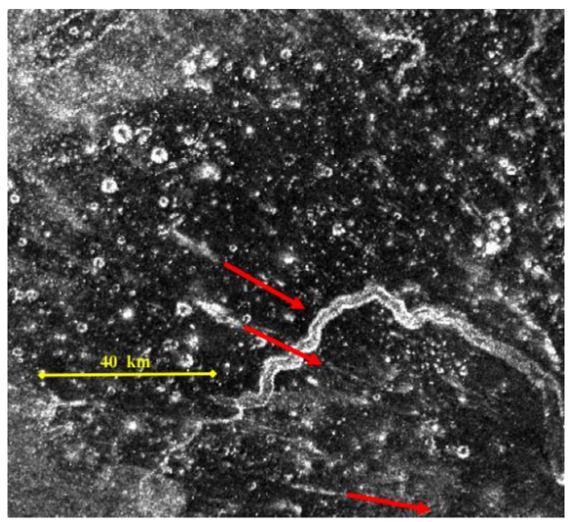

Fig. 1. 12.6 cm Earth-based radar image of the pyroclastic deposit and Schroter's Valley; arrows, from SE ends of three radar-bright streaks, point toward Aristarchus crater [9].

Visible Light: The LROC WAC normalized reflectance mosaic shows diffuse crater-radial bright features. However, the three radar-bright streaks shown in Fig. 1 are not visible in the WAC mosaic, indicating that these streaks are buried beneath the lunar regolith. The NAC images of areas above these streaks display a slightly lower albedo than the surrounding pyroclastic material.

Thermophysical: Diviner-derived temperatures, measured over the lunar night, allow estimation of rock abundances and depths [10]. The cm-scale rocks forming radar-bright streaks show consistent thermophysical signatures. The characteristic H-parameter value for the streaks is ~ 0.06 m, while the highest value for the presumably most uniform, fine-grained parts of the pyroclastic deposit exceeds 0.1 m.

Rocks near the lunar surface warm and cool much more slowly than adjacent fine-grained regolith due to their higher thermal inertia. Bolometric temperatures, measured over the lunar night, can be fit by one-dimensional thermal models, allowing estimation of the vertical thermal inertia profile down to the lunar thermal skin depth [8]. The average surface temperatures of the northern-most two streaks diverge from those of adjacent non-streak areas through the lunar night, reaching about 2 K warmer just before sunrise (Fig. 2), indicating that the rocks forming the streaks lie just above the diurnal skin depth. Streak temperatures are fit well by a thermal model with H = 0.06 m, mixed with an additional half-space representing 0.5 % rocks by volume starting at a depth of 10 cm. Several results from the standard model of Hayne *et al*. [8] with various H-parameter values are shown for comparison. The standard models fit the off-streak data but predict slightly higher temperatures than measured in the early evening for the on-streak data, lending credence to the mixed-rock model.

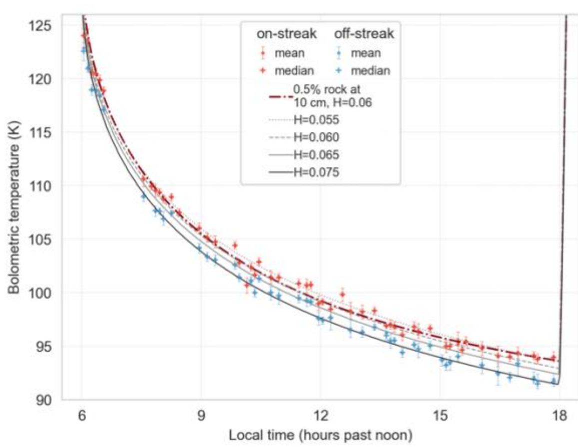

Fig. 2. Average bolometric temperatures on two radar-bright streaks (red), and temperatures for similar areas immediately off the streaks (blue), for the lunar night; red line shows the fit of a mixed-rock thermal model, while results from the standard model without rocks are shown in grey.

This thermal model provides good fit results for 0.5 % by volume of rocks within the thermal skin depth. Additional rocks, buried beneath this depth, may be sensed by radar but do not contribute to the thermal signature.

Discussion: The streaks radial to Aristarchus crater were emplaced immediately after the crater's formation, 130 – 189 my ago. The radar and visible light images, combined with temperature data, indicate that the streaks occur at depths of ~ 10 cm or more below the present surface. These observations indicate that the pyroclastic material was "gardened" by meteorite and micrometeorite impacts sufficiently to emplace at least this depth of regolith over the streaks in less than 200 my.

Fig. 3 compares the result from the current study with a compilation of regolith reworking depths vs. *in situ* exposure ages for selected Apollo cores [1,2]. The current result lies close to the depth/age correlation measured in cores from Apollo 16 and 17.

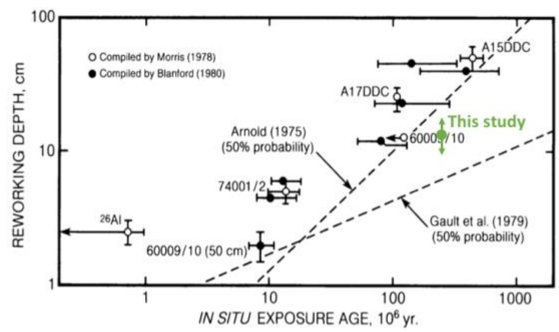

Fig. 3. Depth vs. exposure age for Apollo cores (*Lunar Sourcebook*); green arrow indicates result from this study.

Conclusions: Streaks radial to Aristarchus crater, emplaced in the adjacent pyroclastic deposit, constitute a specific time horizon. Impact-induced mixing in the deposit has gardened material formerly at the surface to a depth of at least 10 cm in the past 130 - 189 my. This rate is in good agreement with the reworking rates calculated from the vertical mixing of regolith in Apollo core samples. These results suggest that evolution rates at the Apollo landing sites are representative of rates at significantly larger scales. While this study is focused on the Aristarchus plateau and one Copernican-aged crater, similar combinations of remote sensing data could be used to estimate regolith evolution rates across the entire lunar surface.

References: [1] Morris, R. V. LPS 9, 1801, 1978. [2] Blanford, G. LPS 11. 1357, 1980. [3] Zanetti M. et al, Icarus DOI 10.1016/j.2017.01.030, 2017. [4] Gaddis L.R. et al, Icarus 161, 262, 2003. [5] Campbell B.A. et al, Geology 208, 135, 2008. [6] Robinson M.S. et al Space Science Rev. 150, 81, 2010. [7] Paige D.A. et al, Space Sci. Rev. DOI 10.1007/s11214-009-9529-2, 2009. [8] Hayne P.O. et al. (2017) J. Geophys. Res., DOI 10.1002/2017JE005387, 2017. [9] Campbell B.A. et al DOI 10.1016/j.icarus.2010.03.011. [10] Bandfield, J.L. et al, J. Geophys. Res. DOI 10.1029/2011JE003866, 2011.